



This is an Accepted Manuscript of an article published by Taylor & Francis in International Journal of Remote Sensing on 29 July 2020, available online: <https://doi.org/10.1080/2150704X.2020.1767822>

Document downloaded from:



Cork oak woodland land-cover types classification: a comparison between UAV sensed imagery and field survey

Florence Heuschmidt^{a*}, David Gómez-Candón^b, Cristina Soares^a, Sofia Cerasoli^a, João M. N. Silva^a

^aForest Research Centre, School of Agriculture, University of Lisbon, Lisbon, Portugal;

^bIRTA Institute of Agrifood Research and Technology, Lleida, Spain

*corresponding author: florence.hj10@gmail.com

Abstract

This work assesses the use of aerial imagery for the vegetation cover characterization in cork oak woodlands. The study was conducted in a cork oak woodland in central Portugal during the summer of 2017. Two supervised classification methods, pixel-based and **object-based image analysis (OBIA)**, were tested using a high spatial resolution image mosaic. Images were captured by an **unmanned aerial vehicle (UAV)** equipped with a **red, green, blue (RGB) camera**. Four different vegetation covers were distinguished: cork oak, shrubs, grass and other (bare soil and trees shadow). Results have been compared with field data obtained by the point-intercept (PI) method. Data comparison reveals the reliability of aerial imagery classification methods in cork oak woodlands. Results show that cork oak was accurately classified at a level of 82.7% with the pixel-based method, and 79.5% with the **OBIA** method. 96.7% of shrubs were identified by the **OBIA** approach whereas there was an overestimation of 21.7% with the pixel approach. Grass presents an overestimation of 22.7% with **OBIA** method and **12.0%** with pixel-based method. Limitations rise from using only spectral information in the visible range. Thus, further research with the use of additional bands (vegetation indices or height information) could result in better **land-cover types** classification.

1. Introduction

The Mediterranean region is one of the most affected by global warming (IPCC 2014). The increasing aridity caused by warming and drought is the main reason for changes in Mediterranean forests structure and function (Peñuelas et al. 2017) and can negatively impact ecosystem services. Cork oak (**Quercus suber L.**) woodlands occupy an important place in western Mediterranean countries, particularly in Portugal (APCOR 2018). It plays an important role in Portuguese economy as well in delivering several ecosystem services as air and water quality, mitigation of climate change and soil protection (Marañón et al. 2012).

Mediterranean cork oak woodlands are forest ecosystems characterized by low tree density and a mixed understory of shrubs and herbaceous vegetation (Acácio and Holmgren 2014). In order to adapt cork oak woodland management to climate change and ensure its sustainability, it is essential to understand the woodland composition and vegetation dynamic with a frequent monitoring of the vegetation cover and structure (Vogiatzakis and Careddu 2003). Vegetation cover maps can describe an ecosystem at a

specific time and allow the analysis of the spatial-temporal changes (Enderle and Weih 2005; Pádua et al. 2017; Sedda, Delogu, and Dettori 2011).

Traditional field inventories are time-consuming, subject to surveyor errors, some methods are destructive and have some limitations to describe forest functions that can only be studied at the landscape scale (Köhl 2013). Thus, field inventories are being replaced gradually by techniques based on aerial imagery data (Baxendale et al. 2016; Surovy, Ribeiro, and Panagiotidis 2018). These techniques can be repeatable and are promising for long-term studies, both on small and large scales (Baxendale et al. 2016; De Luca et al. 2019; Surovy, Ribeiro, and Panagiotidis 2018; Vogiatzakis and Careddu 2003). With an important progress in the development of **unmanned aerial vehicle (UAV)** platforms, sensors and image processing, methods based on aerial imagery are well adapted for medium-size forests monitoring (Pádua et al. 2017). Recent studies show that the use of aerial imagery can be a reliable method for surveying forest ecosystems (Chianucci et al. 2016) including complex Mediterranean forest ecosystems such as cork oak woodlands (De Luca et al. 2019; Surovy, Ribeiro, and Panagiotidis 2018).

The complexity of the study area, with the presence of three layers (cork oak trees, shrubs and grasses) was evaluated to select a suitable classification method. In the literature, several studies claim that the object-based image analysis (OBIA) classification approach outperforms the pixel-based method on aerial images (Franklin 2018; Pande-Chhetri et al. 2017; Sibaruddin et al. 2018) and provides accurate information of cork-oak ecosystems cover (De Luca et al. 2019; Sedda, Delogu, and Dettori 2011). The pixel-based image supervised classification method, which analyses the spectral properties of every pixel, is the most common procedure (Enderle and Weih 2005). However, with this method, the image resolution improvement leads to an increase of intra-class spectral variability leading to a less accurate statistical interpretation between classes (Kim et al. 2011; Yu et al. 2006). The OBIA solves many problems of classification observed in traditional method since it benefits from the local spatial, spectral and textural information present in an image (Gao and Mas 2008; Yu et al. 2006).

The objectives of the study are to compare two image classification methods for the semi-automatic classification of aerial images: pixel-based and OBIA, and to assess their difference from a traditional method based on field survey.

2. Material and methods

2.1. Study area

The study area is located in Central Portugal (39°08'N, 08°19'W) and covered by a Mediterranean cork oak woodland of 84 050 m². The climate is typically Mediterranean with hot and dry summers, while most of the precipitation is concentrated between October and April (Acacio and Holmgren 2014). Cork oak (**Quercus suber L.**) constitutes the tree layer, with a mean height of 7.9 m, and the understory is composed of a mixture of shrubs and herbaceous species. For the shrub *stratum*, the main species are cistus (**Cistus salvifolius**) and ulex (**Ulex airenensis**). The study area was surveyed by an UAV and sampled with a field study cover method using transects covering all the site.

2.2. Images collection and processing

Aerial images were taken on June 9th 2017 with a multicopter UAV named Phantom3 Professional (DJI-Innovations Inc., Shenzhen, China). The auto-stabilizing UAV gimbal was equipped with a built-in visible **red, green and blue** (RGB) spectral bands camera.

RGB images were acquired at fixed waypoints with 80% in-track and 72% cross-track overlap. A single UAV flight was needed to cover the whole study area. It was conducted at 40 m height under clear skies and low wind speed conditions between 12:00 and 14:00 solar time. A total of 353 pictures of 4.94 megabyte each, and with a resolution of 4000 x 3000 pixels have been taken. Image series were saved with Global Positioning System (GPS) coordinates thanks to UAV inertial control system.

Image ortho-rectification, georeferencing and mosaicking (in WGS84 / UTM-29N) were performed with Agisoft Photoscan software (Agisoft LLC, ST. Petersburg, Russia). The obtained orthomosaic has 0.02 m ground sample distance (GSD). Nevertheless, original GSD was resampled to 0.10 m for operational reasons with QGIS 2.16 software that used a **bilinear interpolation method**.

2.3. UAV mosaic classification

In order to describe vegetation cover, four classes were defined as objects in the UAV images: cork oaks, shrubs, grass and other (bare soil and tree shadows). Tree shadows were separated from shrubs and grass since different vegetation covers can be found under the shade of the trees. It was decided to put bare soil and tree shadows together because of the negligible area covered by these two classes. Two supervised methods were tested: a pixel-based approach and an OBIA approach. Traditional methods are pixel based. Nonetheless, OBIA method benefits of the objects spatial, spectral and textural information and thus is more used with high resolution imagery (Gao and Mas 2008). Classifications were performed with the ***k*-nearest neighbours (*k*-NN)** algorithm. In fact, there are several works about classification algorithms comparison in order to find the best for cover mapping. However, their conclusions are not the same (Phan and Kappas 2017). Kim et al. (2012) observed that **support vector machine (SVM)** classifier outperformed the ***k*-NN** classifier. Another work, that investigated six classifiers performance (**naïve bayes (NB)**, **SVM**, ***k*-NN**, **bootstrap-aggregation ensemble of decision trees (BagTE)**, artificial neural network, and deep neural network (DNN)) in Landsat imagery, concluded that all classifiers, with the exception of NB performed similarly. But for edge-pixels, SVM and ***k*-NN** were the best classification methods for Landsat classification (Heydari and Mountrakis 2018). Moreover, nowadays ***k*-NN** method is widely used and its simplicity and accuracy makes it good enough to be taken into account (Fu et al. 2019). The workflow procedure adopted is summarized in Figure 1.

2.3.1. Pixel-based image classification

The pixel-based classification was performed through the open source “Semi-Automatic Classification” plugin of QGIS 2.16 geographic information system, developed by Luca Congedo (2016). The implemented workflow after displaying the RGB 0.10 m resolution image can be divided in two main steps: creation of training areas and image classification.

- (1) A training database was first created to collect the training areas called **regions of interest (ROIs)**. The automatic region growing algorithm was selected to create ROIs. The region growing algorithm consists in choosing manually a pixel of interest (seed) and the algorithm selects adjacent pixels with similar spectral values to the seed pixel (Congedo 2016). Each ROI identifies one of the four

vegetation classes. When classification previews showed good results, training areas were saved, and the procedure continued with the image classification.

- (2) The minimum distance algorithm was applied to assign a class to all pixels in the image by comparing the spectral characteristics of each pixel to the spectral characteristics of reference vegetation cover classes. Thus, the distance is calculated for every pixel in the image, assigning the class of the spectral signature that is closer, according to a discriminant function (Congedo 2016; Richards and Jia 2006).

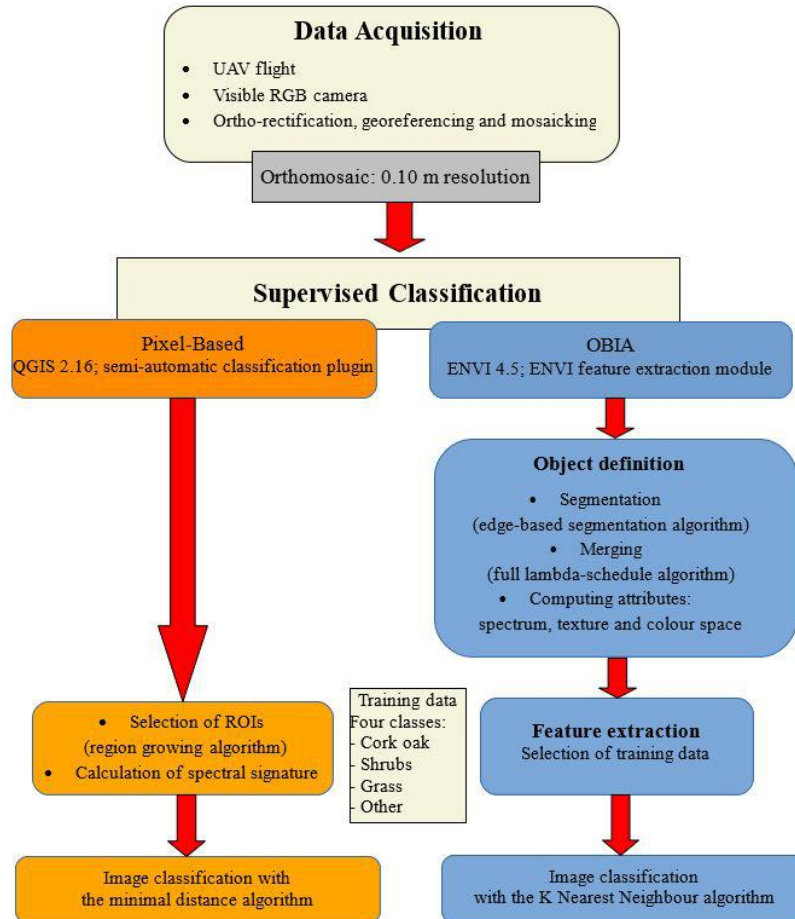


Figure 1. Workflow of the aerial image acquisition and classification with the two supervised methods.

2.3.2. *OBIA classification*

The OBIA method was used in ENVI 4.5 software through the module ENVI Feature Extraction. The classification process is divided into two main steps: defining objects and extracting features. The first step consists in segmenting the image into regions of similar pixels (through segmenting and merging) and computing attributes for each region. The feature extraction step consists in defining the classes and classifying objects. This allows to assign the segments to a class.

- (1) Segmentation is the process of partitioning an image into segments by grouping neighbouring pixels with similar feature values (brightness, texture, colour, etc.). The edge-based segmentation algorithm that only needs the input parameter scale

level was used. Scale level values range from 0 (finest segmentation) to 100 (all pixels grouped into one segment) (ENVI 2008). The best delimiting vegetation objects tested was 40. To each segment is assigned the mean band values of all the pixels that belong to that region.

In order to improve the delineation of vegetation boundaries, the merging segments tool was used. This step allows to aggregate small segments within larger textured areas, following the full lambda-schedule algorithm (ENVI 2008; Robinson, Redding, and Crisp 2002). The merge level parameter ranges from 0 (no merging) to 100 (all segments merged into one). A lambda value of 80 was set.

The final segmented image was partitioned into a total of 32 758 regions. For each one, spectral, texture and colour space attributes were computed. Spectral attributes were computed for each band in the original image. Minimum, maximum, average and standard deviation value of the pixels comprising the region in band were calculated. Concerning texture, the following attributes were computed: average data range, average value, average variance and average entropy value of the pixels comprising the region inside a kernel. For colour space, the hue, saturation, and intensity attributes were computed.

- (2) Training data used to classify the image were built using preselected ROIs. Each class was represented by a variety of regions with different sizes and colours. The classification was performed with the *k*-NN algorithm. The *k* parameter is the number of neighbours considered during classification (ENVI 2008). The default value of 3 was kept.

2.4. Fieldwork: the point-intercept method

To collect the field data of cover estimates, the point-intercept (PI) method was selected because it is a non-destructive method with a good accuracy of cover estimation and not vulnerable to operator bias (Kent and Coker 1992). The PI method is based on sampling data at the interception with plant species at predefined points along a transect (Nunes et al. 2014).

In summer 2017, an area of approximately 84 050 m² was surveyed. The sampling design depicted in Figure 2 was followed to cover the area captured by the UAV mosaic. The PI method, using seventeen 50 m linear transects (around 50 points each, spaced every 1 m) was used. At each point, a 5 mm diameter rod was stuck into the ground in a vertical position. All plant species touching the rod were recorded for subsequent analysis. Data were divided into bare soil, grass and shrubs (differentiated into cistus, ulex or other). The height and diameter (in the direction of the transect and perpendicular to it) of the shrubs was recorded. Information about tree canopy was also recorded, i.e. whether the rod was below the canopy of a cork oak or not.

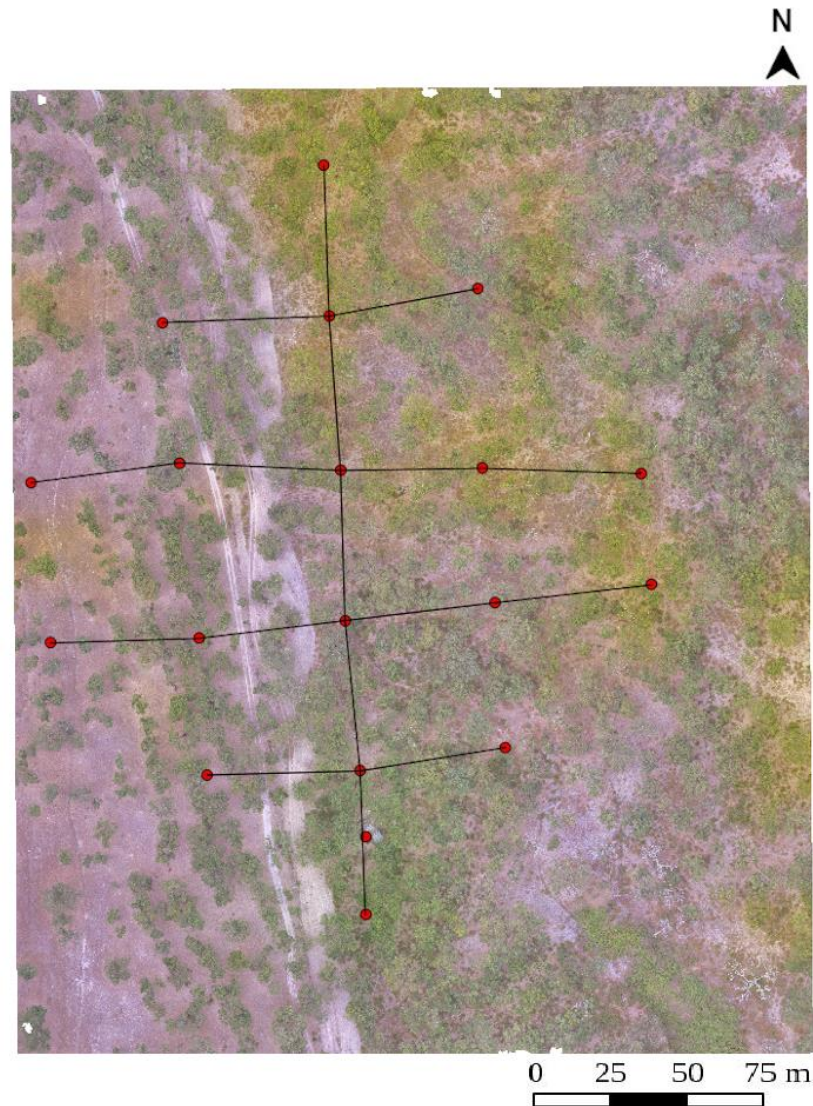


Figure 2. Sampling design overlaying the UAV mosaic. Red dots represent stakes that were used to define the seventeen transects. Five transects were aligned in the north-south direction, and twelve transects were perpendicular to the main direction.

3. Results

3.1. UAV land-cover types classification

Aerial image classifications are shown in Figure 3. In both classifications the dominant vegetation cover class is grass, followed by trees and shrubs, and to a lesser extent by ‘other’ that represents bare soil and tree shadows. The two methods give closer values of cork oak cover than for other vegetation classes. Cork oak cover values ended close to **29.0%** for both methods; **29.8%** for the pixel-based method and **28.7%** for the OBIA method. Larger differences between the two methods can be observed for the shrubs class. It represents **21.9%** of the total cover with the pixel-based method but considerably below this (**17.4%**) regarding the OBIA method. The grass covers less than the half (**45.9%**) of the total surface in the pixel-based map and almost the half (**50.3%**) in the OBIA map.

The class ‘other’ is below **4.0%** of the cover for both classifications (**2.4%** for pixel-based method, **3.7%** for OBIA method).

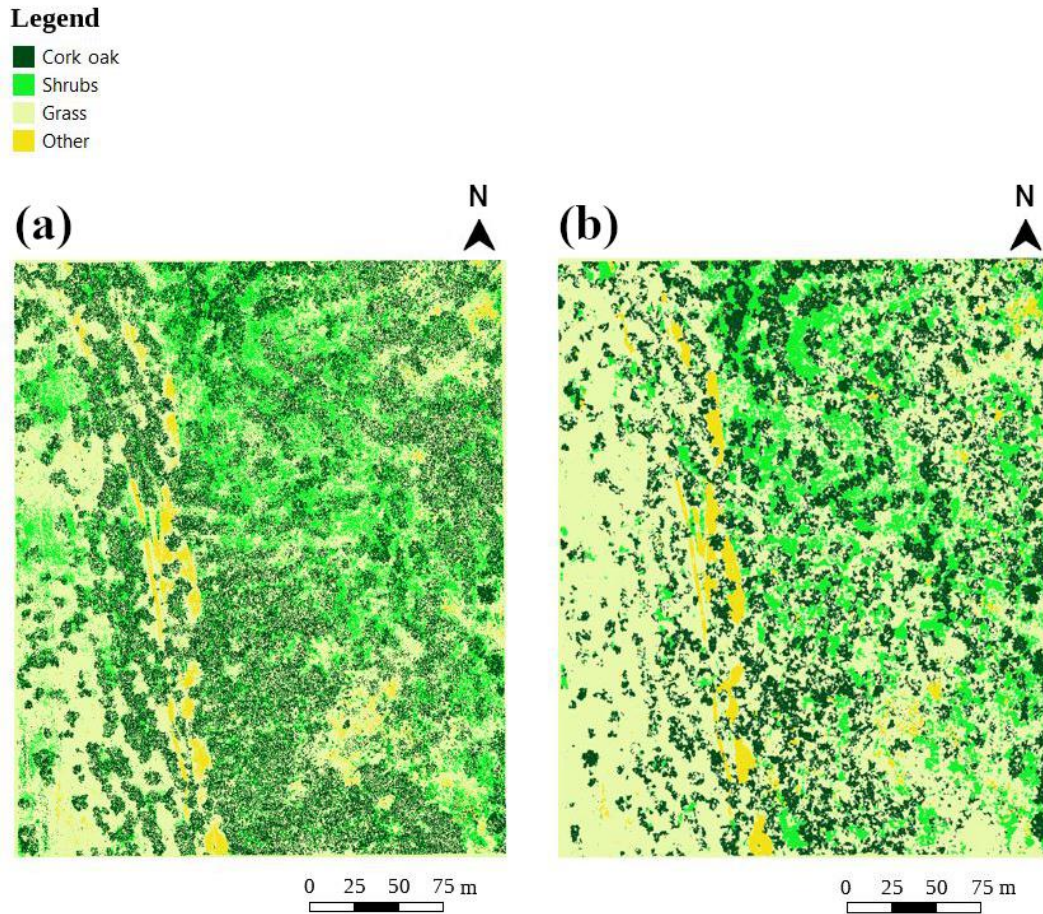


Figure 3. Aerial image classifications performed with the pixel-based method (a) and with the OBIA method (b).

3.2. Comparison with field data

Field results follow the same pattern as both classifications, **41.0%** of the area is covered by grass, **36.0%** is covered by cork oak, **18.0%** by shrubs; and **5.0%** is classified as ‘other’. In order to compare the performance in the area estimation of each class by each classification method, the differences with the field data were computed (Figure 4).

Results show an underestimation of the cork oak trees (**-17.3%** pixel-based, **-20.5%** OBIA) and mostly of ‘other’ (**-51.9%** pixel-based, **-26.1%** OBIA), in opposition to an overestimation of the grass area (**12.0%** pixel-based, **22.6%** OBIA). Shrubs are overestimated by the pixel-based approach (**21.7%**) in opposition to a slight underestimation by the OBIA approach (**-3.3%**). The two methods have the same deviation from the **PI** method for trees, grass and other. This demonstrates the results consistency.

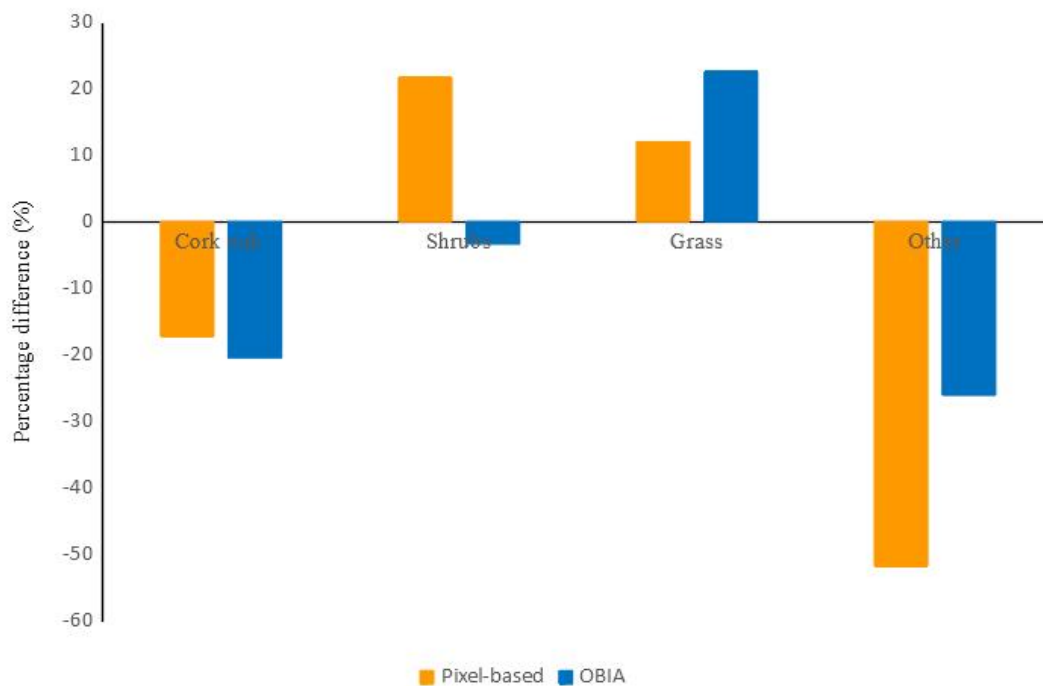


Figure 4. Percentage of under and overestimation of the area of the four vegetation classes obtained by pixel-based approach and OBIA approach, considering the field data as reference.

4- Discussion and conclusion

Results reveal similar usefulness of the methods adopted in this study for vegetation cover classification based on UAV data. The estimates of two image classification methods follow a similar pattern regarding the proportion of the vegetation cover classes when comparing with the estimates from field inventory. However, there are pattern differences regarding cover classes: for three of them (cork oak, grass, other) the results of both methods have the same deviation (under or overestimation), computed as the difference from field results (Figure 4), while larger differences were appreciated for shrubs. It cannot be disregarded that field data can also be subject to human errors (Köhl 2013). However, we consider them as a reference in our analysis, since it allows a comparison between the different methods, useful for a better understanding of the results.

The area covered by cork oak trees estimated by the two classification methods is smaller than the area identified on the field. On the one hand, this difference may be due to an overestimation of the canopy during field work. Indeed, even if a small portion of the tree was above us, it was considered as a canopy presence. Moreover, as a consequence of pruning, it is very common that the internal part of the canopy is less dense than the outer part in cork oaks. This difference in density was not considered in field observations but was captured by aerial images with very high spatial resolution (0.10 m) and considered in automated classification. On the other hand, the image shows that some pixels belonging to the tree canopy are classified as shrubs or grasses. However, we can consider that both classification results are close to field data for trees, with a good ranking percentage of 82.7% with the pixel-based approach and 79.5% with the OBIA approach.

In comparison to the field, the two classification methods overestimate the grass area. The overestimation is bigger with OBIA than with the pixel-based method. With pixel-based method most pixels classified as grass are well classified. The few errors obtained are related to pixels that belong to trees and 'other' classes. With OBIA, there were more misclassified pixels. Indeed, we can assume that pixel-based method is more apt to differentiate the values of the pixels in the canopy area with less dense canopy, whereas OBIA method considers the tree crowns as homogeneous objects.

By comparing the shrub area estimates, an overestimation of 21.7% by the pixel-based and an underestimation of 3.3% by the OBIA approach can be interpreted according to the field results. In the pixel-based approach the overestimation may come from some spectral confusion between vegetation classes. Many pixels belonging to grass and a few pixels belonging to the tree class are classified as shrubs. The error is more visible on the left side of the area (Figures 2 and 3) where the presence of shrubs on the field is low in opposition to the classification by pixel-based approach.

The confusion between the pixels belonging to the grass and those belonging to the shrubs is probably enhanced by the season of the study, summer, and the seasonality of grass and shrubs. The semi-deciduous cistus lost part of the foliage during summer drought period when the fieldwork and UAV flight were conducted, which probably made more difficult to differentiate them spectrally from grass which is also dry in summer. De Luca et al. (2019) shows that better results can be obtained with a **digital surface model** (DSM) that allows a discrimination of two layers using both the height and the normalized difference vegetation index (NDVI), which maximizes the contrast between classes. The use of vegetation indices as NDVI and **normalized difference red edge (NDRE)** index also prove their effectiveness in cork oak distribution maps (Modica, Pollino, and Solano 2019).

The performance of the two methods adopted for classification was compared for the tree main layers (trees, shrubs and grass). The errors in 'other' class are difficult to assess because of their small representativeness of the area. For trees, the pixel-based method is closer to the field value (-17.2%) than the OBIA method (-20.5%). However, the difference between the two methods is very small (3.2%). This difference is around 10.0% for grass, the pixel-based method states an overestimation of 12% and OBIA of 22.7%, and more than 25.0% for shrubs, with a better classification with OBIA than pixel-based (-3.3% and +21,7% respectively compared to field results). Hence, with respect to the field survey, we can conclude that for our study the most efficient method is the OBIA classification. This work highlights the difficulties faced with aerial images classifications on a complex structured ecosystem such as Mediterranean oak woodlands, in which different **land-cover types** can result in similar spectral signature, as observed in shrubs and grasses. Further investigations and tests with additional sensors that have other bands, could improve vegetation cover characterization. The UAV used for this work was equipped with a visible RGB camera only. Literature suggests that in a vegetation structure where different layers have similar shapes and spectral properties, the use of additional bands (e.g. near infrared (NIR), DSM) can be useful for separating two different vegetation layers (Baena et al. 2017; De Luca et al. 2019; Franklin 2018).

Acknowledgements

Authors acknowledge the support of the project MEDSPEC (Monitoring gross primary productivity in Mediterranean oak woodlands through remote sensing and biophysical

modelling, PTDC/AAG-MAA/3699/2014), and the research activities of the Forest Research Centre (UID/AGR/00239/2019) both funded by Fundação para a Ciência e a Tecnologia I.P. (FCT), Portugal, and PORBIOTA (Portuguese E-Infrastructure for Information and Research on Biodiversity (POCI-01-0145-FEDER-022127), supported by Operational Thematic Program for Competitiveness and Internationalization (POCI), under the PORTUGAL 2020 Partnership Agreement, through the European Regional Development Fund (FEDER). FH was funded by the Erasmus+ France program (Erasmus+ traineeship 2017 Mobility Scholarship).

Declaration of interest statement

No potential conflict of interest was reported by the authors.

References

- Acácio, V., and M. Holmgren. 2014. "Pathways for resilience in Mediterranean cork oak land use systems." *Annals of Forest Science* 71 (1): 5-13. doi: 10.1007/s13595-012-0197-0.
- APCOR (Associação Portuguesa da Cortiça) [Portuguese Cork Association] 2018. "Cork Oak Forest." In *Cork*. Santa Maria de Lamas.
- Baena, S., J. Moat, O. Whaley, and D. S. Boyd. 2017. "Identifying species from the air: UAVs and the very high resolution challenge for plant conservation." *PLoS ONE* 12 (11): e0188714. doi: 10.1371/journal.pone.0188714.
- Baxendale, C. L., N. J. Ostle, C. M. Wood, S. Oakley, and S. E. Ward. 2016. "Can digital image classification be used as a standardised method for surveying peatland vegetation cover?" *Ecological Indicators* 68: 150-156. doi: 10.1016/j.ecolind.2015.11.035.
- Chianucci, F., L. Disperati, D. Guzzi, D. Bianchini, V. Nardino, C. Lastri, A. Rindinella, and P. Corona. 2016. "Estimation of canopy attributes in beech forests using true colour digital images from a small fixed-wing UAV." *International Journal of Applied Earth Observation and Geoinformation* 47: 60-68. doi: 10.1016/j.jag.2015.12.005.
- Congedo, L. 2016. "Semi-Automatic Classification Plugin Documentation. Release 6.0.1.1." doi: 10.13140/RG.2.2.29474.02242/1
- De Luca, G., J. M. N. Silva, S. Cerasoli, J. Araújo, J. Campos, S. Di Fazio, and G. Modica. 2019. "Object-Based Land Cover Classification of Cork Oak Woodlands using UAV Imagery and Orfeo ToolBox." *Remote Sensing* 11 (10): 1238. doi: 10.3390/rs11101238.
- Enderle, D. I. M., and R. C. Jr. Weih. 2005. "Integrating Supervised and Unsupervised Classification Methods to Develop a More Accurate Land Cover Classification." *Journal of the Arkansas Academy of Science* 59 (10).
- ENVI. 2008. "ENVI feature extraction Module User's Guide".
- Franklin, S. E. 2018. "Pixel- and object-based multispectral classification of forest tree species from unmanned aerial vehicles." *Journal of Unmanned Vehicle Systems* 6 (4): 195-211. doi: 10.1139/juvs-2017-0022.

- Fu, Y., H. S. He, T. J. Hawbaker, P. D. Henne, Z. Zhu, and D. R. Larsen. 2019. "Evaluating k-Nearest Neighbor (kNN) Imputation Models for Species-Level Aboveground Forest Biomass Mapping in Northeast China". *Remote sensing* 17 (11): 20. doi: 10.3390/rs11172005.
- Gao, Y., and J. F. Mas. 2008. "A Comparison of the Performance of Pixel-Based and Object-Based Classifications over Images with Various Spatial Resolutions." *Online Journal of Earth Sciences* 2 (1): 27-35. Advance online publication. doi: ojesci.2008.27.35.
- Heydari, S. S., and G. Mountrakis. 2018. "Effect of classifier selection, reference sample size, reference class distribution and scene heterogeneity in per-pixel classification accuracy using 26 Landsat sites." *Remote Sensing of Environment* 204: 648-658. doi: 10.1016/j.rse.2017.09.035.
- IPCC (Intergovernmental Panel on Climate Change) 2014. "Climate Change 2014: Synthesis Report." Contribution of Working Groups I, II and III to the Fifth Assessment Report of the Intergovernmental Panel on Climate Change, edited by The Core Writing Team, R. K. Pachauri and L. A. Meyer. IPCC, Geneva, Switzerland, 151 pp.
- Kent, M., and P. Coker. 1992. *Vegetation description and analysis: a practical approach*. Chichester: John Wiley & Sons.
- Kim, J., B. S. Kim, and S. Savarese. 2012. "Comparing Image Classification Methods: K-Nearest-Neighbor and Support-Vector-Machines." *Computer Science*: 133-138.
- Kim, S. R., W. K. Lee, D. A. Kwak, G. S. Biging, P. Gong, J. H. Lee, and H. K. Cho. 2011. "Forest Cover Classification by Optimal Segmentation of High Resolution Satellite Imagery." *Sensors* 11 (2): 1943-1958. doi: 10.3390/s110201943.
- Köhl, M. 2013. "New Approaches for Multi Resource Forest Inventories." In *Advances in Forest Inventory for Sustainable Forest Management and Biodiversity Monitoring*, edited by Corona, P., M. Köhl, and M. Marchetti, 1-16. Forestry Sciences, Springer Science & Business Media.
- Marañón, T., B. Ibáñez, M. Anaya-Romero, M. Muñoz-Rojas, and I. M. Pérez-Ramos. 2012. "Oak trees and woodlands providing ecosystem services in Southern Spain." Paper presented at the conference Trees beyond the Wood, Sheffield, Hallam University (UK), September 5-7.
- Modica, G., M. Pollino, and F. Solano. 2018. "Sentinel-2 Imagery for Mapping Cork Oak (*Quercus suber* L.) Distribution in Calabria (Italy): Capabilities and Quantitative Estimation. " In *New Metropolitan Perspectives*, edited by Calabròlabred by Spina L., Bevilacqua C., 60-67. Springer.
- Nunes, A., S. Tápia, P. Pinho, O. Correia, and C. Branquinho. 2014. "Advantages of the point-intercept method for assessing functional diversity in semi-arid areas." *iForest - Biogeosciences and Forestry* 8 (4): 471-479. doi: 10.3832/ifor1261-007.
- Pádua, L., J. Hruška, J. Bessa, T. Adão, L. M. Martins, J. A. Gonçalves, E. Peres, A. M. R. Sousa, J. P. Castro, and J. J. Sousa. 2017. "Multi-Temporal Analysis of Forestry and Coastal Environments Using UASs." *Remote Sensing* 10 (1): 24. doi: 10.3390/rs10010024.
- Pande-Chhetri, R., A. Abd-Elrahman, T. Liu, J. Morton, and V. L. Wilhelm. 2017. "Object-based classification of wetland vegetation using very high-resolution unmanned air system imagery." *European Journal of Remote Sensing* 50 (1): 564-576. doi: 10.1080/22797254.2017.1373602.

- Peñuelas, J., J. Sardans, I. Filella, M. Estiarte, J. Llusià, R. Ogaya, J. Carnicer, et al. 2017. "Impacts of Global Change on Mediterranean Forests and Their Services." *Forests* 8 (12): 463. doi: 10.3390/f8120463.
- Phan, T. N., and M. Kappas. 2017. "Comparison of Random Forest, k-Nearest Neighbor, and Support Vector Machine Classifiers for Land Cover Classification Using Sentinel-2 Imagery." *Sensors* 18 (1):18. doi: 10.3390/s18010018.
- Richards, J. A., and X. Jia. 2006. *Remote sensing digital image analysis: An introduction*. Berlin: Springer.
- Robinson, D. J., N. J. Redding, and D. J. Crisp. 2002. "Implementation of a fast algorithm for segmenting SAR Imagery." DSTO Electronics and Surveillance Research Laboratory. DSTO-TR-1242, 012-076. Edinburgh, Australia 5111.
- Sedda, L., G. Delogu, and S. Dettori. 2011. "Forty-Four Years of Land Use Changes in a Sardinian Cork Oak Agro-Silvopastoral System: A Qualitative Analysis." *The Open Forest Science Journal* 411 (57): 57-66. doi: 10.2174/1874398601104010057.
- Sibaruddin, H. I., H. Z. M. Shafri, B. Pradhan, and N. A. Haron. 2018. "Comparison of pixel-based and object-based image classification techniques in extracting information from UAV imagery data." *IOP Conference Series: Earth and Environmental Science* 169 (1). doi: 10.1088/1755-1315/169/1/012098.
- Surový, P., N. A. Ribeiro, and D. Panagiotidis. 2018. "Estimation of positions and heights from UAV-sensed imagery in tree plantations in agrosilvopastoral systems." *International Journal of Remote Sensing* 39 (14): 4786-4800. doi: 10.1080/01431161.2018.1434329.
- Vogiatzakis, I. N., and M. B. Careddu. 2003. "Mapping the distribution and extent of *Quercus suber* habitats in Sardinia: A literature review and a proposed methodology." *Geographical Paper* (171).
- Yu, Q., P. Gong, N. Clinton, G. Biging, M. Kelly, and D. Schirokauer. 2006. "Object-based Detailed Vegetation Classification with Airborne High Spatial Resolution Remote Sensing Imagery." *Photogrammetric Engineering & Remote Sensing* 72 (7): 799-811. doi: 10.14358/PERS.72.7.799.